Journal of Applied Electrochemistry **31**: 523–530, 2001.

Electrodeionization 1: Migration of nickel ions absorbed in a rigid, macroporous cation-exchange resin

P.B. SPOOR[1], W.R. ter VEEN[2] and L.J.J. JANSSEN[1]
[1]*Eindhoven University of Technology, Department of Chemical Engineering, Laboratory of Process Development, PO Box 513, 5600 MB Eindhoven, The Netherlands*
[2]*TNO Institute of Environmental Sciences, Energy Research and Process Innovation, Laan van Westenenk 501, PO Box 342, 7300 AH Apeldoorn, The Netherlands*

Received 11 March 2000; accepted in revised form 21 November 2000

Key words: cation exchange, electrochemical ion-exchange, electrodeionization, migration, nickel

Abstract

The removal of nickel ions from a packed bed of ion-exchange material under an applied potential is studied. This process involves the use of an electrodialysis type cell in which the centre compartment is filled with a packed bed of ion-exchange particles. The bed width, concentration of nickel in the resin and electrolyte concentration were varied. Emphasis was placed on the rate of nickel migration, current efficiency and the effective mobility of nickel in the system. The purpose of the study is to aid in the development of a system for the continuous removal of heavy metal ions from dilute solutions.

List of symbols

A	area (m^2)
c	concentration of species (mol m^{-3})
D	diffusion coefficient of species (m^2 s^{-1})
ΔE_{bed}	potential drop across ion-exchange bed (centre compartment) (V)
F	Faraday constant (C mol^{-1})
l	thickness (m)
N	flux of species (mol m^{-2} s^{-1})
n	number of moles species
R	ohmic resistance (Ω)
R	universal gas constant (J mol^{-}1 K^{-1}, V C mol^{-1} K^{-1})
T	temperature (K)
u	mobility (m^2 V^{-1} s^{-1})
X	concentration of fixed sites within ion-exchange resin (mol m^{-3} wet resin)
z	valence (dimensionless)

Greek symbols

ε	fractional pore volume within ion-exchange resin (dimensionless)
η	current efficiency (%)
φ	potential in ion-exchange bed (V)
κ	specific conductivity (Ω^{-1} m^{-1})
ρ	specific flow resistance within ion-exchange resin (Ω C^2 m^{-3})
v	rate at which the centre of gravity of the pore liquid moves (m s^{-1})
ω	charge of fixed sites within ion-exchange resin (dimensionless)

Subscripts

a	anode compartment
av	average
bed	bed of ion-exchange resin occupying centre compartment
c	centre compartment
k	cathode compartment
i	ion
m	membrane
sul	H_2SO_4

Superscripts

–	indicates values within ion-exchange resin
0	initial value at $t = 0$

1. Introduction

Ion-exchange beds and electrodialysis technology are widely used in industry. A hybrid process is being studied in an effort to remove heavy metals from very dilute solutions in a continuous and efficient manner. Other studies have been performed in which the electrolytic regeneration of ion exchangers [1–4] was used in the removal of monovalent metal ions. These ions tend to have a much greater mobility in the exchanger

when compared to bivalent metals such as Ni^{2+} [5–9] and can, therefore, be removed with much greater ease. This work has shown that as nickel was removed from the exchanger and replaced by H^+, the current efficiency for the removal of nickel was gradually reduced and reached a point at which the migration of hydrogen carried nearly 100% of the charge.

The purpose of the present work was to determine the effect of key variables on the behaviour of an ion-exchange resin loaded with nickel ions. One key variable that can be changed without changing the characteristics of the ion-exchanger itself (e.g., degree of cross-linking, concentration of fixed sites) is the concentration of ions in the bed of ion-exchange particles. Another variable is the potential gradient across the bed.

A cell consisting of three compartments separated by ion-selective membranes was used. Experiments were performed to determine the rate of nickel migration in an ion-exchange resin placed in the centre compartment. The strong acid Amberlyst 15 XC-17 macroporous ion-exchange resin with approximately 20% cross-linking was used. This resin was chosen as its high degree of cross-linking minimizes swelling effects. This in turn reduced the pressure drop changes through the ion-exchange compartment, changes in cell resistance due to changes in ionic mobilities and changes in the concentration of fixed sites, X. The migration and diffusion of ions from the outer compartments into the centre compartment and the effect of bed width were also studied.

2. Theory

There are three possible transport paths of an ion through a bed of ion-exchange particles: (i) solely through the resin particles, (ii) alternating through the interstitial solution and the resin particles, and (iii) solely through the interstitial solution. Here the interstitial solution has a very low conductivity, much lower than that of the particles themselves; the first mechanism therefore predominates [10, 11].

The transport of ions through a homogenous bed of ion-exchange resin can be described by the Nernst–Planck relationship [11–13]:

$$N_i = \bar{D}_i \frac{d\bar{C}_i}{dx} + z_i \bar{C}_i \bar{u}_i \operatorname{grad} \varphi + v\bar{C}_i \tag{1}$$

where values inside the resin are denoted with an overbar. The first term on the right hand side describes the diffusion of ion i with concentration $\bar{C}_i$ and diffusion coefficient $\bar{D}_i$. The second term accounts for the migration of ion i with valence state z_i and mobility $\bar{u}_i$. The bed potential gradient is denoted by grad φ. The third term describes the movement of the pore liquid within the ion-exchange particles. The centre of gravity of the pore liquid moves at a rate v which is described by Equation 2:

$$v = \frac{\omega F X}{\rho \varepsilon} \operatorname{grad} \varphi \tag{2}$$

where ρ is the solvent flow resistance of the ion exchanger, X the concentration of fixed sites, ω the charge of the fixed sites and ε represents the fractional pore volume in the ion-exchange resin. The mobility of the ions in the particles, $\bar{u}_i$, is defined by Equation 3:

$$\bar{u}_i = \frac{\bar{D}_i F}{RT} \tag{3}$$

$\bar{D}_i$ is dependent upon the hydration of ion i in the exchanger and the extent of its association with the fixed groups [5]. Some of the main characteristics governing the diffusion coefficient of an ion in an ion-exchange particle are the size and valence of the ion and the degree of cross-linking of the exchanger. The smaller (solvated) ion of lower valence will have the greatest diffusion coefficient in an exchanger with a low degree of cross-linking [6]. Other characteristics such as the exchanger capacity, the concentration of ions in the solution phase, the type of solvent and the co-ions in the system can have varying effects on $\bar{D}$.

In this paper the diffusion and convection terms will be neglected resulting in the following simplified equation [4, 14]:

$$N_i = z_i \bar{C}_i \bar{u}_i \operatorname{grad} \varphi \tag{4}$$

This equation will be used to calculate and compare the nickel mobilities obtained under the various experimental conditions.

3. Experimental details

3.1. *Experimental set-up*

The experimental set-up consisted of a three-compartment Perspex cell and three separate liquid lines (Figure 1). The cell contained two outer compartments with platinum electrodes and a centre compartment that housed the ion-exchange bed. The compartments were separated by a Nafion 117 cation selective membrane on the cathode side and Asahi AMV anion selective membrane at the anode side. The use of an anion selective membrane is possible as it is known to leak protons as well as catalyse the splitting of water [15–17]. The electrolyte circuits connected to the outer compartments had volumes of approximately 500 cm^3 each. The liquid in these circuits was pumped using two Verder V-MD6 type pumps. Liquid was pumped from a 30 dm^3 reservoir through the centre compartment and into a waste container using a Schmitt MP100 pump. The flow rate through the centre compartment was measured using an F&P Co. tube (2-F¼-20-5/36 with glass ball) flow meter. The effective area of the membrane and electrodes inside the cell was 10 cm^2 (1 cm × 10 cm)

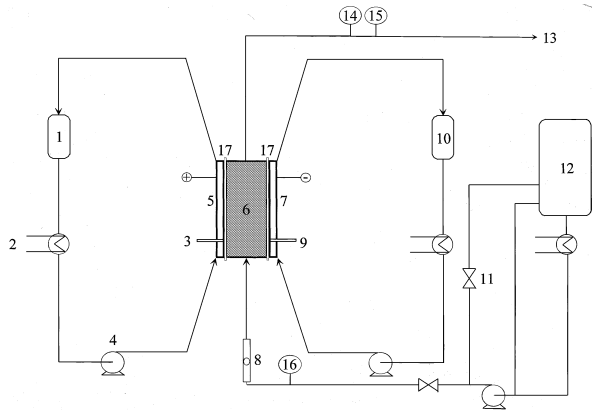

Fig. 1. Experimental set-up (cell enlarged for clarity): (1) anode reservoir; (2) heat exchanger; (3) reference 1; (4) pump; (5) anode compartment; (6) centre compartment; (7) cathode compartment; (8) flow meter; (9) reference 2; (10) cathode reservoir; (11) valve; (12) feed reservoir; (13) to waste container; (14) pH cell; (15) conductivity cell; (16) conductivity cell; (17) ion-selective membrane.

while the volume of the anode, centre and cathode compartments were 5.0 cm^3, 14.6 cm^3 (bed thickness of 1.46 cm) and 5.0 cm^3, respectively. The system was kept at constant temperature (i.e., 298 K) using an M3 Lauda thermostatic bath. Deionized water, prepared using a Millipore Milli-Q water purification system, was used to produce the solutions.

Two conductivity cells were also built into the system, one on the input side and one on the output side of the centre compartment fluid line. Conductivities were measured using a Radiometer (type CDM 2d) conductivity meter. A Philips (PW 9414) pH meter and a Data Precision 2480 voltmeter were also used. The pH and conductivity meters were connected to a Multilab computer interface (built in house) for continuous data acquisition. The Multilab system was also capable of continuous cell potential measurements.

3.2. *Preparation of ion-exchange resin*

Two methods were used in the preparation of the Amberlyst 15 ion-exchange resin. Procedure A, the preparation of resins containing varying concentrations of nickel, involved the following steps, all of which were performed in batch:

(i) Initial regeneration of the exchanger with two bed volumes of 2 M H_2SO_4. This procedure was repeated twice.
(ii) Addition of 2 bed volumes 2 M H_2SO_4 that was allowed to equilibrate with the exchanger over a period of 3 h.
(iii) Rinsing of the exchanger with deionized water until the effluent was pH neutral.
(iv) Equilibration and storage of the exchanger in 2 bed volumes deionized water.
(v) Aliquots (15 cm^3) of this exchanger were then equilibrated with 2 bed volumes of various dilute $NiSO_4$ solutions for a period of approximately three days.
(vi) These samples were then washed and placed in deionized water. Use of the dimethylglyoxime Ni^{2+} indicator showed no nickel in the retinate.

This method is valid as long as the resin effectively absorbs the entire amount of nickel from solution. This is dependent on the equilibrium properties of the material, that is, differences in selectivity between the two ions of interest, but generally occurs when the number of sites available for absorption greatly outnumbers the quantity of nickel in the solution of interest. If this is not the case, the amount of nickel remaining in the solution must be taken into consideration.

Procedure B, the preparation of the resin containing an effective capacity of nickel along with sodium ions, involved steps (i)–(iv) of procedure A followed by the following steps, all of which were performed in batch:

(v) Equilibration of a 200 cm^3 Amberlyst 15 resin sample in the hydrogen form in 2 bed volumes 0.86 M $NiSO_4$ solution for a period of 24 h.
(vi) This solution was neutralized by the dropwise addition of a 4 M NaOH solution and allowed to equilibrate over a period of 14 days.
(vii) The ion-exchanger was then washed and stored in 2 bed volumes deionized water.
(viii) The retinate was analysed for Ni^{2+} using Flame AAS and the concentration of Ni^{2+} in the resin calculated.

Procedure B produced a resin with a nickel concentration of 670 mol m^{-3} wet settled bed. This value was determined by subtracting the quantity of nickel in the retinate from that of the original solution, 0.86 M $NiSO_4$, and dividing by the volume of wet resin.

3.3. *Determination of Na^+ and Ni^{2+} concentrations using 'flame atomic absorption'*

The determination of nickel and sodium concentration in the sample solutions were determined using a Perkin Elmer 3030 atomic absorption system. The absorption is linear between 0 and 1 ppm for sodium and 0 and 2 ppm for nickel. For solutions outside these ranges, dilutions were made using deionized water. The lower detection limit is approximately 4.3×10^{-3} ppm for nickel and 2.0×10^{-4} ppm for sodium with sensitivities of approximately 0.14 and 0.012 for nickel and sodium, respectively. All experiments were performed using an air/acetylene flame and a detection wavelength of 232.0 nm for nickel and 589.0 nm for sodium.

3.4. *Determination of membrane and bed conductivities*

The specific conductivity of the Nafion® 117 cation and Asahi AMV anion selective membranes were determined in order to ascertain their contribution to the ohmic drop of the system as a whole. Before being placed into the cell, the membranes were equilibrated for 24 h with deionized water as received. Two sheets of the same membrane type with an effective area of 10 cm^2 each were clamped into position dividing the cell into three

compartments: anode, centre and cathode. No ion-exchange resin was present in the centre compartment during these experiments. The sulfuric acid solutions placed into each compartment had a concentration of 1 M for each experiment. The solutions were allowed to reach a temperature of 298 K before the measurements were taken. The ohmic drop across the centre compartment including the membranes was determined by placing Luggin capillaries (connected to calomel reference electrodes in concentrated KCl solutions) approximately 2 mm from each membrane in the two electrode compartments. Alternating current impedance measurements were then taken between 1 Hz and 10 kHz at zero direct current. A Solartron 1250 frequency response analyser (FRA) along with the 1286 electrochemical interface was used to perform the impedance analysis. The resistance of the system containing an ion-exchange bed was then measured for comparison. The sulfuric acid solution in the centre compartment was replaced by an Amberlyst 15 ion-exchange bed in the hydrogen form and bordered by Nafion® 117 membranes. Deionized water was cycled through the centre compartment and 1 M H_2SO_4 through the outer compartments at a temperature of 298 K.

3.5. *Electromigration experiments*

3.5.1. *Effect of anode and cathode compartment H_2SO_4 electrolyte concentration*

The effect of acid concentration in the outer anode and cathode compartments was studied. For each run a 300 cm^3 solution containing a predetermined concentration of H_2SO_4 was placed in each of the outer compartments. Solutions in the anode and cathode circuits had a flow rate of approximately 3 $cm^3\ s^{-1}$ each. The system was kept at a constant temperature of 298 K. A run was also carried out in which a 0.5 M Na_2SO_4 solution was placed in the anode compartment while a 1 M H_2SO_4 solution was used in the cathode compartment.

For each run, a new sample of the Amberlyst 15 ion-exchange resin containing nickel and sodium, prepared using procedure B, was placed in the centre compartment between an anion selective (Asahi AMV) at the anode side and cation selective (Nafion® 117) membrane at the cathode side. The anion selective membrane was used to accommodate the migration of anions present in the feed solution in a practical situation and to eliminate the diffusion of Ni^{2+} ions from the centre compartment into the anode compartment. Moreover, it is known that the selectivity of an anion selective membrane is less than 100% and that the transport of H^+ through this membrane is possible. Deionized water was passed 'once through' the ion-exchange compartment at a flow rate of 0.42 $cm^3\ s^{-1}$ while a constant current density of 5.0 mA cm^{-2} was applied across the cell. The following characteristics of the system were monitored: pH and conductivity of the effluent solution; cell voltage; ohmic drop between the reference electrodes; temperature of each solution; volume of the anolyte and catholyte; and flow rate of solution through the centre compartment.

Samples were taken at regular intervals from the anode and cathode compartments and later analysed for Ni^{2+} using the procedure described in Section 3.3.

3.5.2. *Effect of initial Ni^{2+} content in the ion-exchange bed*

A known amount of the resin sample prepared using procedure A was placed into the ion-exchange compartment of the cell between an anion selective (Asahi AMV) at the anode side and cation selective (Nafion® 117) membrane at the cathode side. The anode and cathode compartments were filled with a 1 M H_2SO_4 solution while the ion exchange compartment was supplied by a 30 dm^3 deionized water reservoir at 0.42 $cm^3\ s^{-1}$ in a 'once through' configuration. A constant current density of 25 mA cm^{-2} was applied (supplied by an Autolab system with PG Stat 30 (Eco-Chemie)). The procedure to determine the transport of nickel and the parameters which were monitored during the experiment are given in Section 3.5.1.

3.5.3. *Variation in bed width*

In these experiments the effect of a variation in bed width using the nickel form of the Amberlyst 15 resin from procedure B was studied. The experiment was similar to Section 3.5.1 with the exception that a constant cell voltage of 30 V was applied (Delta Elektronika Power Supply D 050-10) across beds of width 5, 10, 15 and 20 mm. The initial anolyte and catholyte solutions were 0.1 M H_2SO_4.

4. Results and discussion

4.1. *Ohmic resistance of the membranes and ion-exchange bed*

When a 1 M H_2SO_4 electrolyte solution was placed in all three compartments, the cation selective Nafion® 117 membrane was found to have a resistance of 0.07 Ω while the anion selective Asahi Selemion AMV membrane was found to have a resistance of 0.15 Ω.

The specific conductivity of a membrane can be calculated using Equation 5:

$$\kappa_m = \frac{l_m}{R_m A_m} \tag{5}$$

Using a literature value of $l_m = 225\ \mu m$ [18] for the thickness of the Nafion® 117 membrane equilibrated in a 1 M H_2SO_4 solution and a surface area of 0.0010 m^2, the specific conductivity of the membrane at 298 K was found to be 3.02 $\Omega^{-1}\ m^{-1}$. The Nafion® 117 membrane was compared to literature results: Pourcelly et al. calculated a result of 1.8 $\Omega^{-1}\ m^{-1}$ [18]. This agreement is reasonable.

The ohmic resistance of ion-exchange beds containing various quantities of nickel ions was determined. In these experiments a 1 M H_2SO_4 solution was used in the outer compartments as electrolyte while a constant current of 250 mA was applied. By subtracting the anodic and cathodic electrode potentials from the cell voltage, and assuming that no polarization occurs at the membrane surfaces, the ohmic potential drop across the cell, ΔE_{cell}, was obtained. The resistance of the ion-exchange bed was calculated by subtracting the anolyte and catholyte resistance, R_a and R_k, respectively, and both membrane resistances from the total resistance of the cell, R_{cell}.

The ohmic resistance of the bed, R_{bed}, is depicted in Figure 2 against the loading percentage of the resin by nickel ions. R_{bed} at $c_{Ni,c} = 0$ was measured using the procedure outlined in Section 3.4 while all other values were determined from ΔE_{bed} and the applied current at t=0.5 h (to eliminate start-up effects) during the experiments outlined in Section 3.5.2. From this figure it can be seen that R_{bed} increases linearly with increasing Ni^{2+} content. It is assumed that the error which occurs due to the use of the Nafion® membrane resistance when both sides were in contact with a 1 M H_2SO_4 solution, as opposed to the membrane resistance when one side was in contact with a 1 M H_2SO_4 solution and the other with a packed bed of ion-exchange particles with varying ionic content, is relatively small. When one side of the anion exchange membrane is in contact with a 1 M H_2SO_4 solution and the other with a bed of resin particles, no anions can migrate from the central compartment to the anode compartment without water decomposition at the membrane–particle interface. Anion selective membranes are not perfect, however, and can leak protons. It was found that about 1.52×10^{-6} mol s^{-1} H_2SO_4 leaked through the Asahi Selemion AMV membrane when one side was in contact with a 1 M H_2SO_4 solution and the other with a bed of ion-exchange particles. The current efficiency for proton transport through an anion exchange membrane under the fore mentioned conditions is approximately 50% [19, 20]. The resistance of the anion selective membrane when one side is in contact with water and the other with a 1 M sulfuric acid solution is nearly equal to the resistance of the membrane when both sides are in contact with 1 M sulfuric acid.

Since the resin has a much higher conductivity than the deionized water (1.6×10^{-4} Ω^{-1} m^{-1}), almost all current will be transported through it. The effective contact area of the membrane with a bed of ion-exchange resin is smaller than the geometric surface area of the membrane. The current will only be transported across the contact points between the membrane and the resin particles.

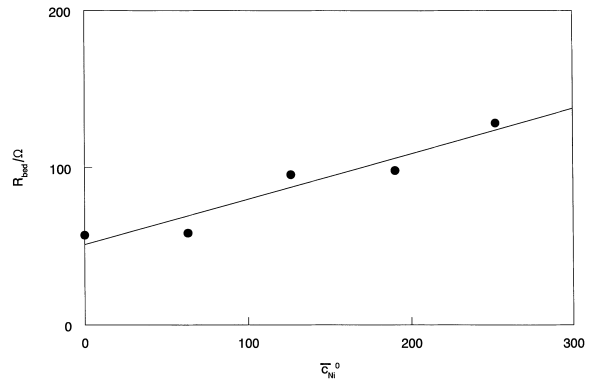

Fig. 2. Ohmic resistance of ion-exchange bed with respect to $\bar{c}^0_{Ni}$.

4.2. *Nickel transport*

4.2.1. *Effect of anode and cathode compartment H_2SO_4 electrolyte concentration*

The effects resulting from the variation of anode and cathode compartment H_2SO_4 concentration ($c_{k,sul}$ and $c_{a,sul}$, respectively) were studied to better understand the cause of pH change in the centre compartment and the effect of an increasing H^+ supply (through diffusion from the outer compartments) to the ion-exchange bed on the flux of nickel ions, N_{Ni}.

The amount of nickel transported into the cathode compartment from a nickel (670 mol m^{-3}) and sodium loaded bed (460 mol m^{-3}, calculated from the capacity obtained from the supplier of the material, 1800 mol m^{-3} fixed ionogenic sites) with respect to electrodialysis time is depicted in Figure 3. From Figure 3 it follows that the H_2SO_4 concentration in the anolyte and catholyte has little influence on the nickel flux at early times ($t < 4$ h). The influence of the H_2SO_4 concentration in the anolyte and catholyte on N_{Ni} increases gradually with increasing time of electrodialysis; at later times it causes the nickel flux to increase with decreasing H_2SO_4 concentration in the outer compartments. It was found that the pH of the centre compartment solution at the outlet of the cell was virtually constant during the course of an experiment but was dependent on the H_2SO_4 concentration in the

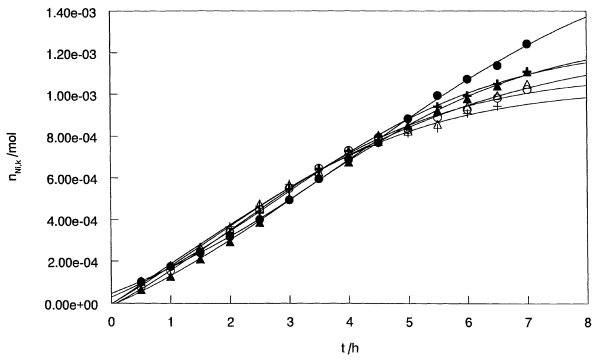

Fig. 3. Nickel content in catholyte as a function of time for the series of experiments in which a bed loaded with nickel and sodium was used and $c^0_{k,sul} = c^0_{a,sul}$ concentrations were varied. A current density of 5.0 mA cm^{-2} was applied. Electrolyte concentrations: (●) 0.5 M Na_2SO_4; (+) 0.9 M H_2SO_4; (△) 0.7 M H_2SO_4; (○) 0.5 M H_2SO_4; 4. (╋) 0.3 M H_2SO_4; (▲) 0.1 M H_2SO_4.

electrode compartments. Figure 4 represents the average concentration of H^+ in the effluent with respect to the initial concentration of sulfuric acid in the anode compartment for the same experiments represented in Figure 3. From Figure 4 it can be seen that upon increased H_2SO_4 concentration in the anode and cathode compartments, where $c_{a,sul}=c_{k,sul}$, the concentration of H^+ in the effluent increased linearly. This corresponds to acid leakage through the membranes.

In the second series of experiments only the anolyte was varied (0.5 M Na_2SO_4, 1 M H_2SO_4 and 0.1 M H_2SO_4) and the catholyte was kept constant (1 M H_2SO_4). The resulting H^+ concentrations in the effluent solutions are also presented in Figure 4. The experiment in which an initial 0.5 M Na_2SO_4 anolyte accompanied a 1 M H_2SO_4 catholyte produced the lowest H^+ concentration in the effluent of the centre compartment. This experiment can also be interpreted as one in which the H_2SO_4 anolyte concentration was virtually zero. The experiment that employed a 0.1 M H_2SO_4 anolyte and 1.0 M H_2SO_4 catholyte produced an effluent pH similar to that produced when both electrolytes were 0.1 M H_2SO_4 solutions. Use of a 1.0 M H_2SO_4 anolyte and 0.1 M H_2SO_4 catholyte produced an effluent pH slightly larger than that of the case when both outer solutions were 0.9 M H_2SO_4 solutions. These three experiments demonstrate the relatively small H_2SO_4 flux from the cathode compartment into the centre compartment solution. The majority of H_2SO_4 present in the centre compartment effluent was transported from the anode compartment. Figure 3 also contains the nickel transport data for the sodium sulphate anolyte. The use of this solution as anolyte produced the lowest nickel flux at early times and the greatest at later times. It also led to the removal of the greatest amount of nickel from the bed after 7 h electrodialysis time. No nickel was removed from the bed due to exchange with the centre compartment solution, as nickel ions were not detected in the effluent solutions of all experiments.

A pixelated pattern of brown spots was observed on the anion selective membrane at the contact points with it and the ion-exchange particles when the sodium sulphate solution was used as anolyte. No discolouration was observed when a 1 M H_2SO_4 anolyte was used. The size and intensity of these spots strongly depended on the H_2SO_4 concentration in the anolyte. The brown spots are likely due to water splitting since the concentration of H^+ is not sufficient to ensure the charge flux imposed by the current across the cell. As the concentration of H_2SO_4 in the anolyte was increased, the anion selective membrane was observed to degrade to a lesser degree.

4.2.2. *Effect of varying initial nickel concentrations in the ion-exchange bed on nickel flux*

To determine the effect of nickel content in the resin on nickel flux, a series of experiments was carried out in which a constant current density of 25 mA m^{-2} was applied to various Amberlyst 15 resin beds of differing nickel and hydrogen contents (prepared using procedure A). 1 M sulfuric acid solutions were placed in the outer compartments while the central compartment was fed with deionized water. The bed was prepared in such a way as to be homogeneous at the beginning of the experiment. In Figure 5 the nickel content in the catholyte is given as a function of the electrodialysis time, t. It can be seen that at the start of the experiment, $t=0$, the catholyte contained a small quantity of Ni^{2+} ions. These ions diffused into the cathode compartment from the bed of ion-exchange particles in exchange for protons. This occurred during the preelectrolysis time, which lasted approximately 0.5 h to ensure constant temperature. From Figure 5 it follows that the quantity of nickel in the catholyte increased linearly with increasing time of electrodialysis, and tapered slightly near the end of the experiment. The average nickel flux, $N_{Ni,av}$, was calculated from the slope of the curves given in Figure 5. It was found to be proportional with $\bar{c}^0_{Ni}$.

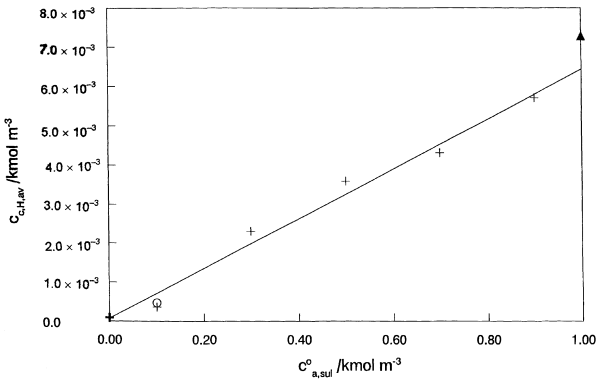

Fig. 4. Average concentration of H^+ ions in centre compartment effluent as a function of anolyte H_2SO_4 concentration. See caption of Figure 3 for experimental details: (+) identical anolyte and catholyte H_2SO_4 concentrations; (○) 0.1 M H_2SO_4 anolyte – 1.0 M H_2SO_4 catholyte; (▲) 1.0 M H_2SO_4 anolyte – 0.1 M H_2SO_4 catholyte; (✙) Na_2SO_4 anolyte – 1.0 M catholyte.

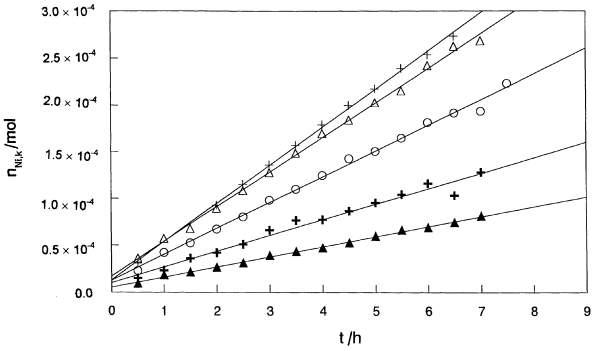

Fig. 5. Nickel content in catholyte over time. Current density 25 mA cm^{-2} for all experiments in this series. 1 M H_2SO_4 anolyte and catholyte solutions. Experiments differed in initial nickel ion concentration in the ion-exchange bed: (+) 319.9; (Δ) 254.6; (○) 191.9; (✙) 127.5; (▲) 64.0 mol m^{-3}.

The average current efficiency for Ni transport, $\eta_{Ni} = 2FN_{Ni,av}Q^{-1}$, also experienced a proportional increase with increasing $\bar{c}^0_{Ni}$. The current efficiencies for all the experiments in this Section were found to be quite low, the lowest being approximately 3% and the highest 10%. The remaining fraction of charge, $1 - \eta_{Ni}$, was carried by hydrogen ions.

The potential difference, ΔE_{bed}, was observed to decrease slightly over time. This was due to the small decrease in the nickel content of the bed.

4.2.3. *Effect of bed width*

The transport of nickel from the Amberlyst resin (procedure B) to the cathode compartment at a constant cell potential for different bed widths with respect to time is shown in Figure 6. The results can be represented by curves with an inflection point and were fitted using Equation 6:

$$n_{Ni,k} = a_1 + \frac{a_2}{1 + \exp\left(-\frac{t-a_3}{a_4}\right)} \quad (6)$$

It can be concluded that Equation 6 fits the experimental results very well. The nickel flux was determined using the derivative of Equation 6:

$$N_{Ni} = \frac{\partial n_{Ni,k}}{\partial t}\left(\frac{1}{A}\right) = \frac{a_2}{a_4}\left[1 + \exp\left(\frac{-(t-a_3)}{a_4}\right)\right]^{-2} \times \exp\left(\frac{-(t-a_3)}{a_4}\right) \quad (7)$$

The initial nickel flux, N^0_{Ni}, was used to determine the mobility of nickel in the resin under the initial conditions. Using Equation 4 along with the initial bed potential gradient, nickel concentration and flux values, the mobility of Ni^{2+}, $\bar{u}^0_{Ni}$, was calculated. The average mobility for all bed widths is given in Figure 7 at $\bar{c}^0_{Ni} = 670$ mol m^{-3}. It was also found that the charge required to remove a given amount of nickel was only slightly affected by the bed width.

5. Discussion

The migration of nickel in an ion-exchange resin was affected by the bed width, concentration of nickel and, to a lesser degree, the electrolyte composition in the anode compartment. The mobility of nickel and hydrogen ions through the resin, the mechanism with which hydrogen was supplied to the bed and the influence of the electrolytes were ascertained from these experiments.

The quantity of nickel ions transported from the ion-exchange bed, uniformly loaded with nickel and sodium prior to electrodialysis, into the cathode compartment over time is given by a sigmoidal curve (Equation 6). Examples of these curves are given in Figures 3 and 6. The inflection occurred only in experiments utilizing a bed loaded with nickel and sodium ions. It is known that the mobility of an ion will increase when in the presence of an ion of higher mobility [11]. The inflection is caused by the difference in the mobility of nickel ions in a bed containing a combination of nickel and sodium, or nickel and hydrogen (the mobility of H^+ being higher than that of Na^+). Before the inflection the flux increased with time, this increase was due to the substitution of Na^+ in the resin with protons from the anode side of the cell.

As the nickel and sodium ions were removed from the ion-exchange bed during electrodialysis, they were replaced by protons from the anode compartment. The mechanism with which these ions were supplied to the bed strongly depended on the concentration of sulfuric acid in the anolyte. At high $c_{a,sul}$ (i.e., > 0.1 M), the diffusion of H^+ ions will predominate. At $c_{a,sul} \approx 0$, the protons were mainly supplied to the bed by the decomposition of water. It is well known [15–17] that the decomposition of water at anion selective membranes containing quaternary ammonium groups occurs at rates much larger than at cation selective membranes containing sulphonic acid groups. The decomposition of

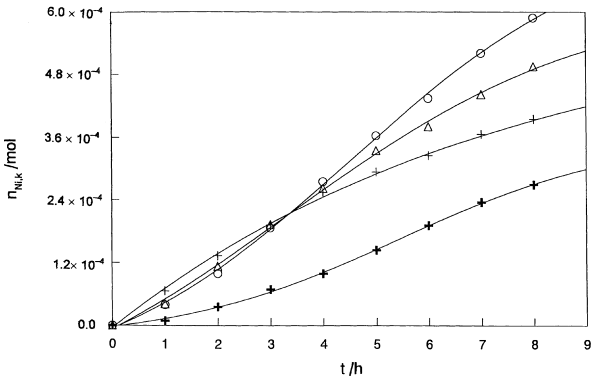

Fig. 6. $n_{Ni,k}$ as a function of time for the series of experiments in which the bed width was varied. A constant applied cell potential of 30 V was applied across beds loaded with nickel and sodium. Data fitted according to Equation 6. Bed width: (+) 5; (Δ) 10; (○) 15; (╪) 20 mm.

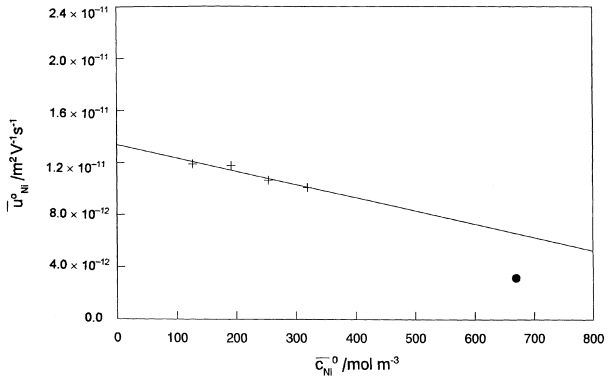

Fig. 7. Initial nickel ion mobilities for the series of experiments in which the nickel content of the resin was varied, $\bar{u}^0_{Ni}$ (+) (see caption of Figure 5 for experimental details); as well as average nickel mobility through beds in nickel and sodium form for the series in which various bed widths were studied (●) (see caption of Figure 6 for experimental details).

water at the membrane-resin interface produces a localized increase in pH within the membrane and causes the membrane to degrade. The quaternary ammonium groups of the Asahi AMV anion selective membrane undergo the Hofmann elimination at high pH [11]. The intensity of the brown spots on the membrane caused by the degradation increased dramatically with decreasing anolyte H_2SO_4 concentration, indicating the increased importance of water decomposition on the regeneration of the bed. A segment of the Asahi AMV membrane was also observed to turn brown in a concentrated NaOH solution.

The diffusion of sulfuric acid into the centre compartment was also observed with increasing $c_{a,sul}$. The increased concentration of sulfuric acid increased the conductivity of the centre compartment solution. This caused a small increase in the fraction of current transported through the centre compartment solution as opposed to the resin. The initial nickel flux, N^0_{Ni}, is an important parameter in determining the industrial possibilities for the use of an ion-exchange resin in this process. N^0_{Ni} increases with increasing potential gradient over the bed, grad φ, and initial nickel concentration in the bed.

The initial mobility of the nickel ions within the ion-exchange resin tended to decrease slightly as the initial nickel content of the bed was increased from approximately 128 to 320 mol m^{-3} (Figure 7). This is in accordance with theory which states that as nickel is replaced by two equivalents of hydrogen, the increased osmotic pressure between the inside of the particle and the bulk solution causes the water content of the resin to increase. The increase in water content of the particle results in an elevated mobility of the nickel ions [11]. As the water content of the Amberlyst 15 ion-exchange resin changed only slightly during the course of the experiment (due to its high degree of cross-linking), the decrease in $\bar{u}_{Ni}$ is small. In Figure 7, the presence of sodium in the resin as opposed to hydrogen is seen to cause a slight decrease in the nickel mobility. This agrees with theory [11]. The current efficiency for all experiments was low. This was due to the presence of the highly mobile H^+ and/or Na^+ ions in the resin.

6. Conclusions

The focus of this study was to examine changes in the Ni^{2+} concentration in the ion-exchange resin, the effect of bed width and the influence of anolyte and catholyte concentrations in both outer compartments on the performance of a cell that couples ion-exchange and electrodialysis. It was found that the resistances of the membranes were small compared to that of the resin. The flux of nickel within the Amberlyst 15 ion-exchange resin was small but the low degree of swelling allowed greater control of the variables of interest. The flux of nickel and the current efficiency for the transport of nickel within the exchanger was found to increase exponentially with Ni^{2+} concentration in the resin. The mobility of nickel in the resin, in agreement with theory, decreased with increasing nickel concentration in the resin. The mobility of Ni^{2+} ions in an aqueous solution, calculated from the limiting equivalent conductance of Ni^{2+} in aqueous solution at 298 K, viz. 5.4×10^{-3} m^2 Ω^{-1} [21], was found to be about 10^3 times higher than the mobility of Ni^{2+} ions adsorbed in an Amberlyst 15 ion-exchange bed.

It was found that the majority of acid leakage originated from the anode compartment and that this flux was linear with H_2SO_4 concentration. The use of Na_2SO_4 as anolyte produced the highest current efficiency and nickel flux. It did, however, cause substantial degradation of the anion exchange membrane.

References

1. E. Korngold, Desalination **16** (1975) S225.
2. W.R. Walters, D.M. Weiser and L.Y. Marek, *Ind. Eng.-Chem.* **47** (1955) 61.
3. V.D. Grebenyuk, N.P. Gnusin, I.B. Barmashenko and A.F. Mazanko, *Russian J. Electrochem.* **6** (1970) 139.
4. H. Neumeister, L. Fürst, R. Flucht and Van Dy Nguyen, *Ultrapure Water* **13** (1996) 60.
5. B.A. Soldano and G.E. Boyd, *J. Am. Chem. Soc.* **75** (1953) 6107.
6. G.E. Boyd and B.A. Soldano, *J. Am. Chem. Soc.* **75** (1954) 6091.
7. E. Heymann and I.J. O'Donnell, *J. Colloid Sci.* **4** (1949) 405.
8. G.E. Boyd and B.A. Soldano, *J. Phys. Chem.* **58** (1954) 456.
9. J.A. Wesselingh, P. Vonk and G. Kraaijeveld, *Chem. Eng. J.* **57** (1995) 75.
10. K. Vuorilehto and A. Tamminen, *J. App. Electrochem.* **27** (1997) 749.
11. F. Helfferich, 'Ion Exchange' (McGraw-Hill, London, 1961).
12. H.M. Verbeek, L. Fürst and H. Neumeister, *Comput. Chem. Eng.* **22** (1998) S913.
13. K.S. Spiegler and C.D. Coryell, *J. Phys. Chem.* **56** (1952) 106.
14. I.W. Cumming, H. Tai and M. Beiev, *Trans. Inst. Chem. Eng.* **75** (1997) 9.
15. M.Taky, G. Pourcelly and C. Gavach, *J. Electroanal. Chem.* **336** (1992) 195.
16. J.J. Krol, M. Wessling and H. Strathmann, *J. Membr. Sci.* **162** (1999) 145.
17. R. Simons, *Desalination* **28** (1979) 41.
18. G. Pourcelly, A. Lindheimer and C. Gavach, *J. Electroanal. Chem.* **305** (1991) 97.
19. J. Molenat, G. Pourcelly, I. Tugas and C. Gavach, *Russian J. Electrochem.* **32** (1996) 170.
20. Y. Lorrain, G. Pourcelly and C. Gavach, *J. Memb. Sci.* **110** (1996) 181.
21. R. Parsons, 'Handbook of Electrochemical Constants' (Butterworths Scientific Publications, London, 1959).